Elsevier Editorial System(tm) for Continental Shelf Research
Manuscript Draft

Manuscript Number:

Title: Geophysical and biological forcing of phytoplankton thin layer variability in Monterey Bay, California

Article Type: Special Issue; Thin Layers

Keywords: phytoplankton, thin layers, fronts, upwelling ecosystems

Corresponding Author: Dr. John Ryan,

Corresponding Author's Institution: MBARI

First Author: John Ryan

Order of Authors: John Ryan; Margaret A McManus; James M Sullivan

Abstract: During the "Layered Organization in the Coastal Ocean" (LOCO) field program in Monterey Bay, California, we integrated intensive water column surveys by an autonomous underwater vehicle (AUV) with satellite and mooring data to examine the spatiotemporal scales and interacting processes of phytoplankton thin layer development. A repeatedly occupied AUV survey track covered inner to outer shelf waters. AUV observations spanned from August 18 to September 6, 2005, with most observations during August 25 - September 1. From 6,841 profiles, we quantified variability in layer prevalence, intensity, and thinness. Thin layer criteria were (1) thickness <= 3 m at the full-width half-maximum, (2) peak chlorophyll at least twice the local background concentrations, and (3) a corresponding peak in optical backscattering. By these criteria 3,978 of the 6,841 profiles (58%) contained thin layers. Thin layers were observed at depths between 2.6 and 17.6 m, and their depths showed diurnal vertical migration of the layer phytoplankton populations. Average layer thickness was 1.4 m, and average intensity was 3.2 x background (13.5 µg l-1 above background). Horizontal scales of thin layer patches ranged from < 100 m to >10,000 m. A thin layer index (TLI) was computed from layer frequency, intensity and

thinness. Maximum spatially-binned average TLI was in mid-shelf waters, coincident with a frontal zone between resident bay waters and an intrusion of low-salinity offshore waters that developed following a wind relaxation/reversal on August 22-25. AUV sections across this front indicated enhanced upward nutrient transport in the front, and satellite observations showed locally enhanced chlorophyll concentrations along the front. Minimum TLI was furthest offshore, in the area most affected by the intrusion of offshore, low-chlorophyll waters into the bay. Following the August 22-25 wind reversal, upwelling winds resumed, and average layer intensity doubled during August 25-29, in parallel with increases in insolation and stratification. The primary nutrient supply mechanism for this thin layer bloom was not wind-driven upwelling, but rather two other processes: internal tidal pumping of nutrient-rich waters from Monterey Canyon onto the northern shelf and vertical circulation in the intrusion frontal zone. Peak TLI was observed on August 29 during a nighttime survey, when the phytoplankton were concentrated in the nutricline, consistent with the observed diurnal vertical migration of dinoflagellates dominated by Akashiwo sanguinea. Empirical orthogonal function decomposition of the thin-layer particle size distribution data from this survey showed that the prevalent dinoflagellate size class observed, having a cross-sectional dimension peak at ~ 50 μm that is consistent with Akashiwo cells, dominated thin layers throughout the inner to outer shelf survey domain. During a subsequent wind relaxation and reversal August 30 - September 1, thin layer frequency increased by ~1/3 while intensity decreased by ~1/3. This wind forcing resulted in a stronger intrusion of low salinity waters into the study region, reduction of vertical density stratification by > 50%, and nearly complete disappearance of thin layers by September 6.

Geophysical and biological forcing of phytoplankton thin layer variability in Monterey Bay, California

John P. Ryan[1], Margaret A. McManus[2], James M. Sullivan[3]

[1]*Monterey Bay Aquarium Research Institute, 7700 Sandholdt Road, Moss Landing, California 95039 USA*
[2]*University of Hawaii at Manoa, Department of Oceanography, 1000 Pope Road, Honolulu, Hawaii 96822 USA*
[3]*University of Rhode Island, Graduate School of Oceanography, South Ferry Road, Narragansett, Rhode Island 02882 USA*

Corresponding author:
John Ryan
Phone: (831) 775-1978
Fax: (831) 775-1620
ryjo@mbari.org

Abstract

During the "Layered Organization in the Coastal Ocean" (LOCO) field program in Monterey Bay, California, we integrated intensive water column surveys by an autonomous underwater vehicle (AUV) with satellite and mooring data to examine the spatiotemporal scales and interacting processes of phytoplankton thin layer development. A repeatedly occupied AUV survey track covered inner to outer shelf waters. AUV observations spanned from August 18 to September 6, 2005, with most observations during August 25 – September 1. From 6,841 profiles, we quantified variability in layer prevalence, intensity, and thinness. Thin layer criteria were (1) thickness <= 3 m at the full-width half-maximum, (2) peak chlorophyll at least twice the local background concentrations, and (3) a corresponding peak in optical backscattering. By these criteria 3,978 of the 6,841 profiles (58%) contained thin layers. Thin layers were observed at depths between 2.6 and 17.6 m, and their depths showed diurnal vertical migration of the layer phytoplankton populations. Average layer thickness was 1.4 m, and average intensity was 3.2 x background (13.5 $\mu g\ l^{-1}$ above background). Horizontal scales of thin layer patches ranged from < 100 m to >10,000 m. A thin layer index (TLI) was computed from layer frequency, intensity and thinness. Maximum spatially-binned average TLI was in mid-shelf waters, coincident with a frontal zone between resident bay waters and an intrusion of low-salinity offshore waters that developed following a wind relaxation/reversal on August 22-25. AUV sections across this front indicated enhanced upward nutrient transport in the front, and satellite observations showed locally enhanced chlorophyll concentrations along the front. Minimum TLI was furthest offshore, in the area most affected by the intrusion of offshore, low-chlorophyll waters into the bay. Following the August 22-25 wind reversal, upwelling winds resumed, and average layer intensity doubled during August 25-29, in parallel with increases in insolation and stratification. The primary nutrient supply mechanism for this thin layer bloom was not wind-driven upwelling,

but rather two other processes: internal tidal pumping of nutrient-rich waters from Monterey Canyon onto the northern shelf and vertical circulation in the intrusion frontal zone. Peak TLI was observed on August 29 during a nighttime survey, when the phytoplankton were concentrated in the nutricline, consistent with the observed diurnal vertical migration of dinoflagellates dominated by *Akashiwo sanguinea*. Empirical orthogonal function decomposition of the thin-layer particle size distribution data from this survey showed that the prevalent dinoflagellate size class observed, having a cross-sectional dimension peak at ~ 50 μm that is consistent with *Akashiwo* cells, dominated thin layers throughout the inner to outer shelf survey domain. During a subsequent wind relaxation and reversal August 30 – September 1, thin layer frequency increased by ~1/3 while intensity decreased by ~1/3. This wind forcing resulted in a stronger intrusion of low salinity waters into the study region, reduction of vertical density stratification by > 50%, and nearly complete disappearance of thin layers by September 6.

Keywords: phytoplankton, thin layers, fronts, upwelling ecosystems

1. Introduction

1.1 Environmental Setting

Monterey Bay, California (Figure 1) is a dynamic and productive coastal ecosystem in the central California Current System (CCS). Nutrient-rich waters supporting high primary productivity are upwelled by regional wind forcing of both coastal upwelling and Ekman pumping, and by internal tidal forcing of transport from Monterey Canyon (Figure 1) onto the shelf (Reid et al., 1958; Barber and Smith, 1981; Shea and Broenkow, 1982; Breaker and Broenkow, 1994; Rosenfeld et al., 1994). Bay waters are a mixture of colder, saltier upwelled water and warmer, fresher offshore waters of the California Current (Graham and Largier, 1997). The bay environment significantly changes intermittently with highly variable influxes of these primary source waters.

The intensity and biological consequences of coastal upwelling in this region are greatest between March and November (Pennington and Chavez, 2000). Within this period, circulation and water mass distributions respond rapidly to changes in wind forcing. Equatorward winds produce cold filaments of upwelled waters north and south of the bay, and the upwelling from Point Año Nuevo, 27 km north of the bay, often flows southward across the mouth of the bay (Rosenfeld et al., 1994). A cyclonic gyre forms in the northern bay as a dynamic response to active upwelling (Breaker and Broenkow, 1994). This circulation transports nutrient-rich upwelled waters into the bay and creates a phenomenon known as the 'upwelling shadow', in which residence time and thermal stratification are enhanced (Graham and Largier, 1997). Periods when equatorward winds decrease in intensity (< 3 m s^{-1}) or reverse to poleward are termed 'relaxation events'. During relaxation events, offshore low-salinity waters are rapidly transported shoreward (Bolin and Abbott, 1963; Broenkow and Smethie, 1978; Rosenfeld et al., 1994; Ramp et al., 2005). These low salinity waters are warm relative to recently upwelled

waters but may be cool relative to bay waters that have warmed during residence in the upwelling shadow. Observed responses to relaxation events include rapid flushing of much of the bay by intrusions of offshore low-salinity waters containing relatively low phytoplankton biomass (Ryan et al., 2008a; 2008b), as well as mixing and destratification of the inner shelf water column (Storlazzi et al., 2003).

Previous studies in Monterey Bay have described aspects of phytoplankton ecology relevant to the present study. Multiple studies have shown that the upwelling shadow functions as a dinoflagellate "red tide" bloom incubator (Ryan et al., 2005; 2008b; 2008c; Rienecker et al., 2008; Kudela et al., 2008). Multiple studies have also shown that frontal zones formed by influxes of both upwelled and offshore waters are important sites for aggregation of diatom and dinoflagellate biomass as well as phytoplankton thin layer formation by vertical shear (Pennington and Chavez, 2000; Ryan et al., 2005a; 2008a; 2008b; 2008c; Rienecker et al., 2008).

1.2 Research Objectives

The objectives of this research were (1) to advance measurements of the spatial and temporal variability in phytoplankton thin layers, and (2) to enhance our understanding of the interacting physical, chemical and biological processes that control thin layer development. While intensive optical and acoustic profiling of the shallow northern shelf water column (~ 20 m water depth) was being conducted in northeastern Monterey Bay, we applied a multidisciplinary autonomous underwater vehicle (AUV) to survey the water column of inner to outer shelf waters (20 – 200 m depth). The mooring array and AUV survey locations are shown in Figure 1. Repeated synoptic mapping by AUV provided a key observational capability for understanding the scales and processes of thin layer development and quantifying how layer attributes at the inner shelf array compared with those further offshore.

2. Methods

2.1 Dorado autonomous underwater vehicle (AUV) surveys

The MBARI AUV *Dorado* repeatedly occupied a triangular survey track (Figure 1) during the period August 18 – September 6, 2005. The survey was comprised of two cross-shelf transects and one along-shelf transect, with one of each type of transect extending away from the LOCO primary mooring array site (Figure 1). Of the 20 repeated surveys, 18 were conducted over an 8-day period, between August 25 and September 1, for the purpose of high-resolution thin layer quantification. The other two surveys, one on August 18 and the second on September 6, were for the purpose of thin layer characterization before and following the intensive AUV observation period. In total, 6,841 AUV profiles were made along the survey track.

At a speed of ~1.5 m s^{-1} and a 30° pitch through sequential "saw tooth" profiling, the AUV provided synoptic high-resolution sections through shelf waters. A single transit around the 38 km triangular survey track (Figure 1) averaged 342 profiles in ~6.5 hours. The AUV was equipped with physical, chemical and optical sensors. We present observations from five sensors: (1) a SeaBird SBE 25 CTD that measured temperature and conductivity, (2) a Paroscientific 8CB/4000-I pressure sensor, (3) a HOBI Labs HS-2 sensor that measured optical backscattering at two wavelengths and chlorophyll fluorescence, (4) an *in situ* ultraviolet spectrophotometer (ISUS) sensor that measured nitrate concentrations (Johnson and Coletti, 2002), and (5) a Sequoia Scientific LISST-100 (Laser In Situ Scattering and Transmissometer) that measured the particle size distribution between 1 and 250 μm. The LISST-100 has proven effective for studying the patchiness and evolution of coastal ocean dinoflagellate and diatom blooms (Rienecker et al., 2008).

2.2 Quantification of thin layer attributes

Quantification of thin layer attributes from the AUV data was consistent with the methods

applied to data collected by other researchers using autonomous moored profilers at the main LOCO array site. Specifically, we cross-calibrated AUV fluorometric chlorophyll with that from the moored profiler systems and applied the same thin layer detection and quantification methods (Sullivan et al., this issue). The criteria used for thin layers were: (1) intensity of the chlorophyll layer peak must be at least twice the local background chlorophyll concentration; (2) the fluorometric chlorophyll peak must coincide with a local peak in optical backscattering, to ensure that the fluorescence profile structure is not due simply to vertical variability in the quantum yield of fluorescence; (3) layer thickness at the full-width half-max (FWHM) must be <= 3 m. Layer intensity was quantified as the intensity of the chlorophyll peak above the local background, using a linear baseline method (Sullivan et al., this issue). Here we term this intensity measurement: chlorophyll line height (CLH). Once the AUV data set was reduced into statistics of the time, location {x,y,z}, thickness and intensity of thin layers, further statistical characterizations were computed. To examine spatial patterns, average layer attributes were computed within along-track spatial bins. Bin boundaries were defined from 10 evenly spaced latitude bands spanning the 16.3 km north-south extent of the survey (Figure 1). To examine temporal patterns, average layer attributes were computed for each survey. One additional measure was computed from spatially and temporally binned statistics: a multi-parameter thin layer index (TLI), computed as the product of frequency, intensity and thinness. Thin layer patches were defined as clusters of adjacent profiles in which thin layers were consistently detected. The horizontal scales of the 440 detected patches were computed from the along-track distance spanned by each cluster of thin layer profiles.

To characterize the phytoplankton populations in the thin layers, we analyzed the particle size distribution (PSD) data from the LISST-100 using empirical orthogonal function (EOF) decomposition. This method has previously been applied in Monterey Bay phytoplankton bloom

studies (Rienecker et al., 2008). We present EOF results for the survey having the highest TLI.

2.3 Long-term moorings

To describe oceanographic and atmospheric variation we used measurements from three long-term moorings (Figure 1), one in northern shelf waters (M0), one in the central bay mouth (M1), and one 30 km west of the bay mouth (M2). Mooring observations presented in this study include winds at M2, which represent wind forcing of the greater CCS, and salinity and temperature at M1 and M0, which provide indications of regional water mass changes. Surface wind speed and direction at M2 were measured by a RM Young model 05103 wind monitor. Temperature and salinity at M1 and M0 were measured by Sea-Bird microcat conductivity, temperature, depth (CTD) sensors. CTD data used in this study were averaged from measurements at 3.5, 10 and 20 m depth at each mooring.

2.4 MODIS satellite data

To examine synoptic patterns relevant to water mass and phytoplankton distributions, we used MODIS (Moderate Resolution Imaging Spectroradiometer) satellite data. From Level 1A data we produced true color, chlorophyll fluorescence line height (FLH; Letelier and Abbott, 1996), chlorophyll concentration, and sea surface temperature (SST) images using the SeaDAS software. Processing used calibrations for ocean remote sensing developed by the MODIS Ocean Biology Processing Group. The true color images use the 645 nm (red), 555 nm (green) and 469 nm (blue) bands, having spatial resolutions of 250, 500 and 500 m, respectively, with application of a basic atmospheric scattering correction. For the atmospheric correction required to derive products (FLH, chlorophyll and SST), we computed true 250-m aerosol retrievals using the 859 nm band and a fixed aerosol model (Franz et al., 2006). Resulting image data were mapped to a cylindrical projection. The true resolution of FLH, chlorophyll and SST images are at best ~ 1 km at nadir; bilinear interpolation was used to generate 500 m resolution images. A

previous study (Ryan et al., 2008b) and this study have shown better spatial coverage of parameter retrieval for Monterey Bay from FLH than from chlorophyll images. Therefore, we present true color, FLH and SST imagery to describe synoptic physical and bio-optical patterns.

3. Results and Discussion

3.1 Environmental Variability

Between mid-August and early September 2005, oscillations of upwelling (equatorward) and downwelling (poleward) winds forced transport and mixing of regional water masses and changes in bay water properties. Two wind relaxation events developed during the intensive AUV operational period, August 22–25 and August 30–September 2 (Figure 2a). Each relaxation event was followed by intrusion of low salinity waters onto the northern shelf (Figure 2b; decreases in M0 salinity > 0.1 psu beginning on 8/23 and 9/3). The low salinity intrusion that followed the wind relaxation of August 22–25 (Figure 2a) was most pronounced at mooring M0 during August 24–26 (Figure 2b). The low salinity intrusion that followed the wind relaxation of August 30–September 2 (Figure 2a) resulted in a lower salinity anomaly of longer duration at M0 (Figure 2b).

Propagation of the first low-salinity intrusion into the study domain during late August was observed by AUV volume surveys (Figure 3). By August 25, the low salinity waters occupied a significant portion of the southern AUV survey domain (Figure 3a). The intrusion submerged beneath warm surface waters while spreading northward (Figure 3a-e) and reached the furthest inner shelf waters surveyed and the LOCO array by August 29 (Figure 3e). Vertical motions relevant to phytoplankton ecology were indicated in the salinity and temperature fields. The coldest waters reached the shallowest depth in the frontal zone, where the salinity distributions indicated horizontal interleaving (white + signs in Figure 3a-b).

MODIS satellite imagery acquired on August 25 showed sharp contrast between the bio-optical conditions of northern and southern Monterey Bay (Figure 4a,b). Blue waters of low phytoplankton chlorophyll fluorescence line height (FLH) occupied the southern bay, while green-brown waters of much higher phytoplankton FLH occupied the northern bay. This indicates predominant intrusion into the southern bay of low salinity offshore waters, which are lower in phytoplankton abundance than resident bay waters, very similar to a previous study (Ryan et al., 2008a). The frontal boundary, oriented northwest-southeast, exhibited patchy, locally enhanced color and FLH (Figure 4a,b). The highest FLH and strongest water coloration were in nearshore waters, inshore of the LOCO array and the AUV survey track (Figure 4a,b). Within the frontal zone between the intruding offshore waters and resident bay waters was the coolest SST in the domain (Figure 4c). An AUV survey on this day showed that the leading edge of the low-salinity intrusion was cooler and more weakly stratified than the resident bay waters (Figure 3a). This cool/fresh anomaly was also measured at mooring M0 on August 25 (Figure 2b,c). The cool SST observed by MODIS was not due to advection of recently upwelled water into the bay, which would have caused a high-salinity anomaly rather than the observed low-salinity anomaly. The coincidence of shallow, cold water with salinity interleaving in the frontal zone (white + signs in Figure 3a,b) suggests that the cool SST band was caused by vertical circulation in the front.

3.2 Thin layer statistics

Of the 6,841 water column profiles acquired by the AUV, 58% (n=3,978) contained phytoplankton layer structures that met all thin layer criteria. This percentage is similar to that found from moored profiling time-series at the LOCO array site (56%; Sullivan et al., this issue). The depths of AUV-detected thin layer peaks ranged between 2.6 and 17.6 m. The overall mean thin layer intensity was 13.5 $\mu g\ l^{-1}$ above background (a factor of 3.2 times the background), and

mean thickness was 1.4 m. Cumulative frequency distributions (Figure 5) show that layer vertical scale (thickness) was the most evenly distributed layer attribute, while layer horizontal scale had the most skewed distribution. The horizontal scales of the 440 thin layer patches ranged from < 100 m to > 10,000 m; the median patch size was 320 m. The largest patch, exceeding 10 km, was mapped along the southernmost segment of the offshore AUV transect (Figure 1) on August 27. Median layer statistics computed from the full AUV data set are similar to those quantified from moored profiling time-series at the LOCO array site (Sullivan et al., this issue). Median thickness was exactly the same (1.3 m). Intensity was slightly higher for the AUV data set (2.8x versus 2.5x), consistent with the finding of higher average layer intensity seaward of the array (Section 3.3).

3.3 Spatial variation in average thin layer statistics

Average layer attributes exhibited significant spatial heterogeneity (Figure 6). The frequency of thin layer detection (Figure 6a) ranged from 27% to 81%, with more frequent presence seaward of the shallow-water LOCO array, and the maximum between the 50 and 75 m isobaths. The lowest frequencies were at the southern limit of the survey, over Monterey Canyon (Figure 1), the location that would have been affected longest and most by the low salinity, low FLH intrusion (Figures 3, 4). Average layer intensity ranged between 9.1 and 14.9 $\mu g\, l^{-1}$ above background (Figure 6b). The highest average intensities were observed in two areas of the inner shelf (< 25 m depth, west and southeast of the array), and in mid-shelf waters (south of the array between the 50 and 75 m isobaths). Average layer thickness (Figure 6c) ranged between 1.2 and 1.6 m. In general, layers were thinner in deeper waters. The multi-parameter thin layer index (TLI, Figure 6d) showed that overall, thin layers were most frequent, intense and thin in the upper water column of the mid-shelf (the zone between the 50 and 75 m isobaths). This same zone also exhibited the maximum salinity variance in the upper 20 m (Figure 6e). This high

salinity variance was caused by the influx of a low-salinity intrusion and mixing of water masses in a frontal zone (Figure 3; Section 3.1).

3.4 Diurnal variation in thin layer depth

The average depth of the thin layers exhibited diurnal variation (Figure 7). Layers were on average about twice as deep and in waters 1°C colder during the night as they were during the day. The populations were nearest the surface between ~ 10 am and 2 pm. This characterization of diurnal vertical migration throughout the AUV survey domain is consistent with the description of this process at the LOCO array site, as well as the vertical migratory capabilities of the dinoflagellate that dominated the phytoplankton assemblage during this period, *Akashiwo sanguinea* (Donaghay et al., Sullivan et al., and Rines et al, this issue).

3.5 Temporal variation in thin layer development relative to environmental variation

Thin layer attributes averaged for each of the 20 laps around the triangular survey (Figure 1) exhibited patterns related to the changing meteorological forcing and oceanographic conditions. Thin layer encounter frequencies were very low during the preliminary survey on August 18 and the final survey on September 6 (Figure 8a). During the intensive AUV survey period, August 25 - September 1, thin layer encounter frequency was mostly > 50%. Average layer thickness was < 2 m for all surveys, except for the final survey on September 6 when frequency was also at a minimum (1%). Average layer intensity rose to a maximum between August 25 and 29, ranging from ~7.1 to 19.4 $\mu g\ l^{-1}$ above background (Figure 8b). The multi-parameter thin layer index (TLI) peaked on August 29, when intensity was at its peak, thickness was near the minimum, and frequency was near the maximum (open symbols in Figure 8a,b). Minimum TLI was observed in the September 6 survey, when water column salinity was lowest (M0 in Figure 2b) following the August 30 – September 2 wind relaxation event (Figure 2a). In addition to phytoplankton community changes that would have accompanied water mass

intrusion, shallow density stratification (as in Figure 8d) decreased by more than 50% between September 1 and 6, which would have affected planktonic biological-physical interactions.

The strongest trend in thin layer attributes during the intensive AUV survey period was an increase in layer intensity during August 25-29. This approximate doubling of thin layer intensity coincided with a similar ~50% increase of average chlorophyll concentrations in the upper 20 m (Figure 8c). Increases in thin layer intensity were evident at all spatial bins (bin locations shown in Figure 6) except for the southernmost area seaward of the frontal zone (Figure 4). These results suggest a northern shelf bloom dominated by thin-layer forming phytoplankton. The biological trends corresponded closely with physical trends. During the rise in average chlorophyll and thin layer intensity, vertical density stratification between 3 and 15 m increased by 44% (Figure 8d). The role of increasing stratification in the development of dinoflagellate blooms has been previously observed in Monterey Bay (Ryan et al., 2005). This stratification change was caused primarily by near-surface warming and simultaneous cooling at 15 m (Figures 3; 8d). Salinity at these depths showed opposite trends, with decreasing salinity at 3 m (due to the intrusion; Figure 3) and increasing salinity at 15 m (not shown). These conditions would favor dinoflagellates that can migrate vertically to acquire nutrients in the nutricline. Additionally, PAR was at a maximum during August 26-30 (Figure 2a), supporting greater capacity for photosynthesis.

In examining temporal variability, it is important to evaluate the possibility of survey time affecting thin layer detection and quantification, which would be important for vertically migrating thin layer populations. The times of the AUV surveys are shown in Figures 2 and 8. For the intensive survey period between August 25 and September 1, the first survey in each daily series was started at approximately the same time. For August 26 – September 1, each day was a sequence of two or three laps starting at approximately the same time. Therefore, we

conclude that our results showing the increase in average thin layer intensity during August 25-29 was a biological event and not an artifact of variability in daily sampling periods.

3.6 Synoptic patterns at the peak of thin layer intensity

The peak of thin layer intensity and TLI occurred on August 29 (open symbols in Figure 8a,b). Synoptic bio-optical, nutrient and physical conditions from the AUV survey having the peak average intensity and TLI are shown in Figure 9. This survey started shortly after sunset. The thin layers were consistently detected at the nutricline (Figures 9a,b) and were more consistently aligned with the nutricline than the thermocline (Figures 9a-c). This indicates that vertical migratory behavior of the phytoplankton responded to nutrient concentrations and was critical to determining the depth and intensity of thin layers throughout the AUV survey domain, as shown clearly from moored observations at the LOCO array (Donaghay et al. and Sullivan et al., this issue). The subsurface minimum in nitrate evident throughout the domain (Figure 9b) was unlike the salinity distribution (not shown), suggesting that nutrient uptake by the vertically migrating populations may have created the subsurface nitrate minimum.

3.7 Particle size distributions in thin layers

The dominance of *Akashiwo sanguinea* during this bloom was indicated by observations at the LOCO array site, and the average cross-sectional dimension of *A. sanguinea* cells measured microscopically was ~ 50 μm (Rines et al., this issue). Laboratory and field tests have shown that for populations of dinoflagellates whose cells are pseudo-spherical, the LISST-100 instrument produces a single peak at the average cross-sectional dimension (Rienecker et al., 2008). At the peak of thin layer intensity (Figure 9a), the particle size distribution (PSD) within thin layers was dominated by cells having a cross-sectional length scale consistent with that of *A. sanguinea*. The first EOF of the thin layer PSD data, accounting for 97% of the variance, exhibited a peak at 50 μm (Figure 10). This particle size dominance was prevalent throughout

the intensive AUV time series of August 25 - September 1. These results, together with the observations of vertical migration (Figure 7) and aggregation on the nutricline during the night (Figure 9), indicate that throughout the inner to outer northern shelf survey domain, vertically migrating *Akashiwo* were the dominant phytoplankton creating intense thin layers.

3.8 Processes of nutrient flux to the study area during thin layer intensification

A phytoplankton bloom during late August is indicated by the doubling of thin layer intensity that coincided with a 50% increase in average chlorophyll concentrations in the upper 20 m (Figure 8c). The increase in stratification coincident with the bloom (Figure 8c,d) would presumably favor vertically migrating dinoflagellates that can access nutrients in the thermocline. The decrease in temperature at 15 m during the bloom (Figure 8c,d, and increase in salinity not shown) is consistent with increased nutrient availability in the thermocline. Nitrate concentrations were low in the upper 10 m, reaching nearly 0 in the subsurface nitrate minimum (Figure 9b). We hypothesize that physical mechanisms of nutrient supply contributed to bloom development, and we examine potential processes. We did not measure nutrient uptake by phytoplankton or its variability. Thus, these results are intended only to evaluate the primary nutrient supply mechanisms to the study region.

3.8.1 Nutrient supply by wind-driven upwelling

The period of thin layer intensification during August 25-29 corresponded with the return of upwelling favorable winds (Figure 2a). However we find no evidence of the influx of wind-driven upwelling into the study domain. The salinity increase observed at both M0 and M1 between August 25-27 was accompanied by warming, whereas recently upwelled waters would result in cooling. The cold signature of an upwelling filament was evident only at the mouth of the bay during August 27-28 (M1 in Figure 2c). No cold pulse was observed at the northern shelf mooring (M0 in Figure 2c). Further, no cold/saline upwelling filament was observed to

cross the seaward boundary of the AUV survey during the bloom period (Figure 3). The first clear satellite SST image following the return of upwelling on August 26 was on August 29, at the peak of the bloom. This image showed no evidence of either advection of an upwelling filament into the northeastern bay or local wind-driven upwelling along the bay's northern coast. Therefore, wind-driven upwelling does not appear to have been a factor in nutrient supply to the northern shelf while the phytoplankton bloomed and thin layers intensified.

3.8.2 Nutrient supply by internal tidal pumping

The AUV volume series reveals boluses of relatively cold, saline water in the lower water column of the inner shelf (Figure 3). These patterns are consistent with a physical process known to transport nutrients from Monterey Canyon onto the shelf, internal tidal pumping (Shea and Broenkow, 1982). This process was observed with repeated AUV surveys (Figure 11). Three consecutive surveys showed high nitrate water moving northward below the thermocline into shallow northern shelf waters during a single semidiurnal tidal cycle (Figure 11a inset), reaching the LOCO mooring array site. This nutrient transport pattern was observed through other tidal cycles, including a series of sections along the offshore AUV transect. These observations are consistent with decreasing temperature and increasing salinity and nutrient availability in the thermocline during the bloom, while thin layers and surface warming intensified. Although observed along sections in this and previous studies, the spatial scales of this mechanism of nutrient supply and dependence of its variability on regional wind forcing, circulation, and tidal forcing have not been adequately quantified. Intensive observation and numerical simulations are required to better understand the consequences of this nutrient supply mechanism for the ecosystem.

3.8.3 Nutrient supply by frontal dynamics

As described in section 3.1, the coldest waters (< 11°C) reached the shallowest depth in

the frontal zone as cool filaments extended up into the areas of salinity interleaving (white + signs in Figure 3a-b). Also, the deepest penetration of low salinity waters occurred along the leading (northward flowing) edge of the front. The apparently opposing displacements of shallow low salinity waters downward and deeper cold waters upward in the frontal zone indicate enhanced vertical circulation in the front. Satellite images showed enhanced chlorophyll FLH along the front (Figure 4), consistent with aggregation of motile phytoplankton in a convergence zone (Ryan et al., 2005; 2008b; 2008c). The highest TLI and salinity variance were observed where this frontal zone exhibited the strongest vertical displacements (Figure 3a,b; Figure 6 d,e). Thus, the patterns observed by in situ and remote sensing indicate enhanced vertical circulations in the frontal zone, which may have enriched nutrient supply for phytoplankton growth (Figure 6b). Layer thinness (Figure 6c) may have also been enhanced by vertical shear in the front. The role of vertical shear in thin layer development has been observed within this type of frontal zone in Monterey Bay for non-motile phytoplankton populations (Ryan et al., 2008a).

3.9 Implications for harmful algal bloom (HAB) ecology

The 2005 LOCO array site was located in shallow waters of northeastern Monterey Bay upwelling shadow, a region known to incubate, spread and retain dinoflagellate blooms (Ryan et al., 2005; 2008b; 2008c; Rienecker et al., 2008; Kudela et al., 2008). Some of the dinoflagellates found in this region of Monterey Bay, including *Alexandrium catanella* and *Dinophysis sp.* (Ryan et al., 2008c), can cause harm through production of toxins. *Cochlodinium cf fulvescens*, which has been a significant bloom former in this region since 2004 (Curtiss et al., 2008; Kudela et al., 2008; Ryan et al., 2008b), can cause fish and shellfish mortality events. *Akashiwo sanguinea*, the dinoflagellate that dominated thin layer variability during the 2005 LOCO study, has been recently linked to a previously unknown harmful effect. External coating of seabirds by

organic matter from an *Akashiwo* bloom in Monterey Bay impaired the insulating function of feathers, causing bird morbidity and mortality by hypothermia (Jessup et al., in revision). The LOCO 2005 study connects thin layer ecology of vertically migratory dinoflagellates to understanding HABs that develop from dinoflagellate populations, which are favored by the stratified environment of the Monterey Bay upwelling shadow. Linkages between thin layers and harmful diatom species has already been examined for this region of Monterey Bay. Intense concentration of toxin-producing *Pseudo-nitzschia* populations in subsurface thin layers has been observed in this region and hypothesized as a mechanism for 'cryptic' harmful algal blooms (McManus et al., 2008).

Conclusions

Advances in understanding of thin layer ecology have been possible only with advances in the technologies required to observe complex coastal ocean environments with multidisciplinary sensor suites at sufficient spatial and temporal resolution. Moored profiling systems have enabled great advancements in thin layer studies, and the moored systems applied at the primary LOCO mooring array site provided thoroughly detailed environmental and biological characterization for understanding thin layer variability and processes at that site. In addition, high-resolution measurements by mobile platforms capable of synoptic, multidisciplinary surveys are key to advancing understanding of thin layer ecology in heterogeneous, rapidly changing coastal environments. Dinoflagellate population dynamics dominated the thin phytoplankton variability at the mooring array site during the 2005 LOCO study. AUV mapping across the shelf showed that the same species dominated thin layers from inner to outer shelf waters, and that the most intense and thin phytoplankton layers having the largest horizontal scales were observed seaward of the main mooring array site. Frontal

dynamics may have augmented thin layers in these waters by affecting not only nutrient supply to the vertically migrating phytoplankton populations, but also by aggregation of biomass in a convergent flow and by vertical shear that can intensify layer thinness. Additionally, internal tidal forcing supplied nutrients to the entire study domain, including the mooring array site, in a way that would favor the vertically migrating populations. Interpretation of the voluminous data collected by such advanced moored and mobile observing platforms also requires information on regional meteorological and oceanographic variability. Satellite imaging of the region and moored observations extending from the eastern boundary current system into the bay were essential elements of the observing system that supported understanding of coupled atmosphere-ocean dynamics forcing the development of thin phytoplankton layers in this highly complex environment.

Acknowledgments

This research was supported by ONR grant N00014-04-1-0311 and by the David and Lucile Packard Foundation. We thank MBARI AUV operations personnel H. Thomas, D. Conlin and D. Thompson, and R/V Zephyr and R/V Robert Gordon Sproul personnel who supported AUV operations. M0 mooring data were provided by the Center for Integrated Marine Technology under NOAA award NA160C2936. MODIS data were provided by the Level 1 and Atmosphere Archive and Distribution System (LAADS), and our MODIS data processing was enabled by the NASA MODIS Ocean Biology Processing Group and the NASA SeaDAS software development team.

References

Barber R.T., Smith, R.L., 1981. Coastal upwelling ecosystems, p. 31-68. In Longhurst, A.R.

(Ed.), Analysis of Marine Ecosystems, Academic.

Bolin, R.L., Abbott, D.P., 1963. Studies on the marine climate and phytoplankton of the central coastal area of California, 1954-1960. California Cooperative Oceanic Fisheries Investigations 9:23-45.

Breaker, L.C., Broenkow, W.W., 1994. The circulation of Monterey Bay and related processes. Oceanography and Marine Biology: An Annual Review 32:1-64.

Broenkow, W.W., Smethie, W.M., 1978. Surface circulation and replacement of water in Monterey Bay. Estuarine and Coastal Marine Science 6:583-603.

Curtiss, C.C., Langlois, G.W., Busse, L.B., Mazzillo, F., Silver, M.W., 2008. The emergence of Cochlodinium along the California Coast (USA). Harmful Algae 7:337-346.

Donaghay, P.L., et al., The role of physical, chemical and biological interactions in controlling the formation of thin layers by vertically migrating dinoflagellates in northeastern Monterey Bay, CA, this issue.

Franz, B.A., Werdell, P.J., Meister, G., Kwiatkowska, E.J., Bailey, S.W., Ahmad, Z., McClain, C.R., 2006. MODIS Land Bands for Ocean Remote Sensing Applications, Proc. Ocean Optics XVIII, Montreal, Canada, 9-13 October 2006.

Graham W.M., 1993. Spatio-temporal scale assessment of an 'upwelling shadow' in northern Monterey Bay, California. Estuaries 16, 83-91.

Graham W.M., Largier J.L., 1997. Upwelling shadows as nearshore retention sites: the example of northern Monterey Bay. Continental Shelf Research 17, 509-532.

Jessup, D.A., Miller, M.A., Ryan, J.P., Nevins, H.M., Kerkering, H.A., Mekebri, A. Crand, D.B., Johnson, T.A., Kudela, R.M., 2008. Mass stranding of marine birds caused by a surfactant-producing red tide. PLOS, in revision.

Johnson, K.S., Coletti, L.J., 2002. In situ ultraviolet spectrophotometry for high resolution and

long term monitoring of nitrate, bromide and bisulfide in the ocean. Deep-Sea Research I 49, 1291-1305.

Kudela, R.M., Ryan, J.P., Blakely, M.D., Lane, J.Q., Peterson, T.D., 2008. Linking the physiology and ecology of *Cochlodinium* to better understand harmful algal bloom events: a comparative approach. Harmful Algae, *7*, 278-292.

Letelier, R.M., Abbott, M.R., 1996. An Analysis of Chlorophyll Fluorescence Algorithms for the Moderate Resolution Imaging Spectrometer (MODIS). Remote Sens. Environ. 58, 215-223.

McManus, M.A., Kudela, R.M., Silver, M.W., Steward, G.F., Donaghay, P.L., Sullivan, J.M., 2008. Cryptic Blooms: Are Thin Layers the Missing Connection? Estuaries and Coasts: J CERF DOI 10.1007/s12237-007-9025-4.

Pennington J.T., Chavez, F.P., 2000. Seasonal fluctuations of temperature, salinity, nitrate, chlorophyll and primary production at station H3/M1 over 1989-1996 in Monterey Bay, California. Deep-Sea Research II 47, 947-973.

Ramp, S.R., Paduan, J.D., Shulman, I., Kindle, J., Bahr, F.L., and Chavez, F.P., 2005. Observations of upwelling and relaxation events in the northern Monterey Bay during August 2000. J. Geophys. Res. 110, C07013, doi:10.1029/2004JC002538.

Reid, J.L., Roden, G.I., Wyllie, J.G., 1958. Studies of the California Current System. California Cooperative Oceanic Fisheries Investigations, Progress Report, 1 July 1956 – 1 January 1958, pp. 27-56.

Rienecker, E.R., Ryan, J.P., Marin III, R., Blum, M., Dietz, C., Chavez, F.P., 2008. Synoptic mapping of the phytoplankton size distribution, with applications to the ecology of red tides and harmful algal blooms, Limnology and Oceanography: Methods 6, 153-161.

Rines, J., et al., Fine scale temporal and spatial variability in phytoplankton composition in Monterey Bay, CA., this issue.

Rosenfeld, L.K., Schwing, F.B., Garfield, N., Tracy, D.E., 1994. Bifurcated flow from an upwelling center: a cold water source for Monterey Bay. Continental Shelf Research 14:931-964.

Ryan, J.P., Dierssen, H.M., Kudela, R.M., Scholin, C.A., Johnson, K.S., Sullivan, J.M., Fischer, A.M., Rienecker, E.V., McEnaney, P.R., Chavez, F.P., 2005a. Coastal ocean physics and red tides: an example from Monterey Bay, California. Oceanography 18, 246-255.

Ryan, J.P., McManus, M.A., Paduan, J.D., Chavez, F.P., 2008a. Phytoplankton thin layers in Monterey Bay, California. Marine Ecology Progress Series, 354, 21-34.

Ryan, J.P., Fischer, A.M., Kudela, R.M., Gower, J.F.R., King, S.A., Marin, R. III, Chavez, F.P., 2008b. Influences of upwelling and downwelling winds on red tide bloom dynamics in Monterey Bay, California. Continental Shelf Research, in press.

Ryan, J.P., Gower, J.F.R., King, S.A., Bissett, W.P., Fischer, A.M., Kudela, R.M., Kolber, Z., Mazzillo, F., Rienecker, E.R., Chavez, F.P., 2008c. A coastal ocean extreme bloom incubator. Geophysical Research Letters, 35, L12602, doi:10.1029/2008GL034081.

Storlazzi, C.D., McManus, M,.A., Figurski, J.D. 2003. Long-term, high-frequency current and temperature measurements along central California: insights into upwelling/relaxation and internal waves on the inner shelf. Continental Shelf Research 23: 901-918.

Sullivan, J.S., et al., Coastal thin layer dynamics: consequences to biology and optics, this issue.

Figure Captions

Figure 1. Map of the study region, Monterey Bay, California. The triangular track over the northern shelf in the bay shows the AUV survey path that was repeatedly occupied. The AUV track is 38 km along-track and spans 16.3 km north-south; 7 km east-west. Data from the M0-2 moorings provided data on variability in wind forcing and oceanic conditions; mooring depths are 70 m (M0), 1,000 m (M1) and 1,825 m (M2). The 3 black circles in the northeastern bay show the locations of the LOCO primary mooring sites.

Figure 2. Meteorological and oceanographic variability during LOCO 2005; mooring locations are shown in Figure 1. Time is GMT. (a) Wind velocity at mooring M2 and photosynthetically available radiation (PAR) at mooring M1. Winds were smoothed with a 5-hour running mean. PAR is daily-integrated for the photoperiod, smoothed with a 3-day running mean. Average (b) salinity and (c) temperature in the upper 20 m at moorings M0 and M1. Black bars along the top in (a) and bottom in (c) indicate periods when the AUV was surveying along the track shown in Figure 1; bar length indicates 1, 2 or 3 consecutive laps of the AUV track in a single, continuous survey. Gray bars above the black bars in (c) identify the laps for which salinity and temperature are shown in Figure 3.

Figure 3. Water mass variability resulting from changes in wind forcing during the experiment. High-resolution volume maps are from the times indicated by the gray bars along the bottom of Figure 2c. View is from the south (Figure 1). The depth range of the data shown is 2 to 60 m. White + symbols in (a) and (b) indicate features described in the text (Sections 3.1 and 3.8.3).

Figure 4. MODIS satellite imagery showing water mass distributions and frontal patterns. Images are from August 25, 2005, the peak of a wind relaxation event (Figure 2a), when intrusion of low-salinity offshore waters into Monterey Bay was in progress (Figure 3a). Shown are (a) true-color, (b) chlorophyll fluorescence line height (FLH), and (c) sea surface temperature

(SST). Mooring and AUV survey locations, as in Figure 1, are shown. The vectors at moorings M1 and M0 represents the shallowest measured average velocity during August 23-25, 10 m at M0 and 20 m at M1.

Figure 5. Cumulative frequency distributions of thin layer attributes for the full AUV data set, computed from 3,978 thin layer profiles (Section 2.2). CLH is chlorophyll line height, a measure of layer intensity above the local background. The median for each parameter is marked by a diamond on the x-axis.

Figure 6. Average spatially binned thin layer attributes, computed from 6,841 AUV profiles, 3,978 of which contained thin-layer structures, from 20 repeated surveys along the track shown in Figure 1. Frequency is the percent of profiles containing phytoplankton thin layer structures. CLH is chlorophyll line height, a measure of layer intensity above the local background, and TLI is a normalized multi-parameter thin layer index (Section 2.2). V(S) is the variance in salinity within the upper 20 m. Isobaths are shown in gray in all panels, with isobath depths (m) noted in (a).

Figure 7. Diurnal variability in average thin layer depth and temperature within 4-hour windows, computed from all 3,978 thin layer profiles.

Figure 8. Temporal variability in thin layer attributes relative to background conditions. Each point represents an average for a single iteration of the track shown in Figure 1; time is GMT. (a) layer frequency (percent of profiles having thin layer structures) and thickness; (b) layer intensity (CLH) and the normalized multi-parameter thin layer index (TLI) (Section 2.2); (c) layer CLH relative to average chlorophyll concentrations in the depth range 2-20 m; (d) temperature at 3 and 15 m depth, and the density difference between 15 and 3 m depth. Time series in (c) and (d) were smoothed with a 3-point running mean. Open symbols in (a) and (b) indicate the survey having the maximum TLI, i.e. the most frequently encountered, intense, thin

layer structures. Bio-optical, nutrient and physical conditions during this TLI peak survey are shown in Figure 9.

Figure 9. Chlorophyll, nitrate and temperature along the AUV survey track, for the lap when the average multi-parameter thin layer index (TLI, Section 2.2) reached its maximum value (open symbols in Figure 8a,b). The survey began at (local time) 8:05 pm (after sunset) on August 28 and finished at 2:35 am on August 29. The white contour in all panels is the same reference nitrate isopleth (3 μM).

Figure 10. First empirical orthogonal function (Section 2.2) of the particle size distribution for all phytoplankton thin layers detected in the survey shown in Figure 9. The concentration peak represents the maximum concentration detected in all thin layer profiles from this survey.

Figure 11. Illustration of northward nutrient flux below the thermocline caused by internal tidal pumping from Monterey Canyon. The vertical sections of nitrate were consecutively mapped on August 28-29. The segment of the full AUV survey shown is indicated in the upper-left inset. The inset in (a) shows bottom pressure from an ADCP on the shelf, illustrating the semidiurnal tidal oscillations (gray line) and the start of the consecutive AUV surveys (black circles).

Figure 1

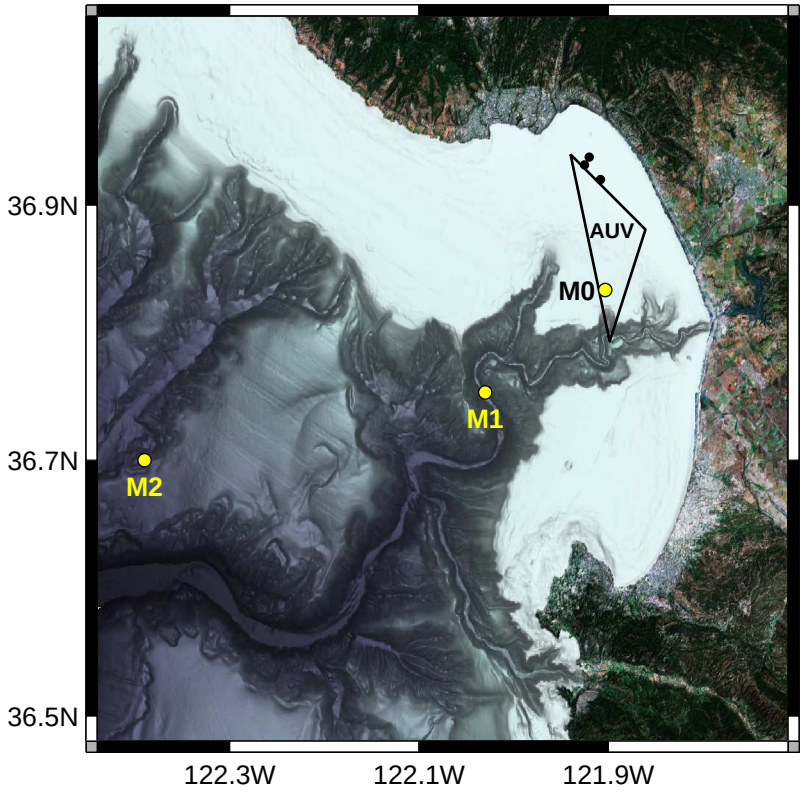

Figure 2

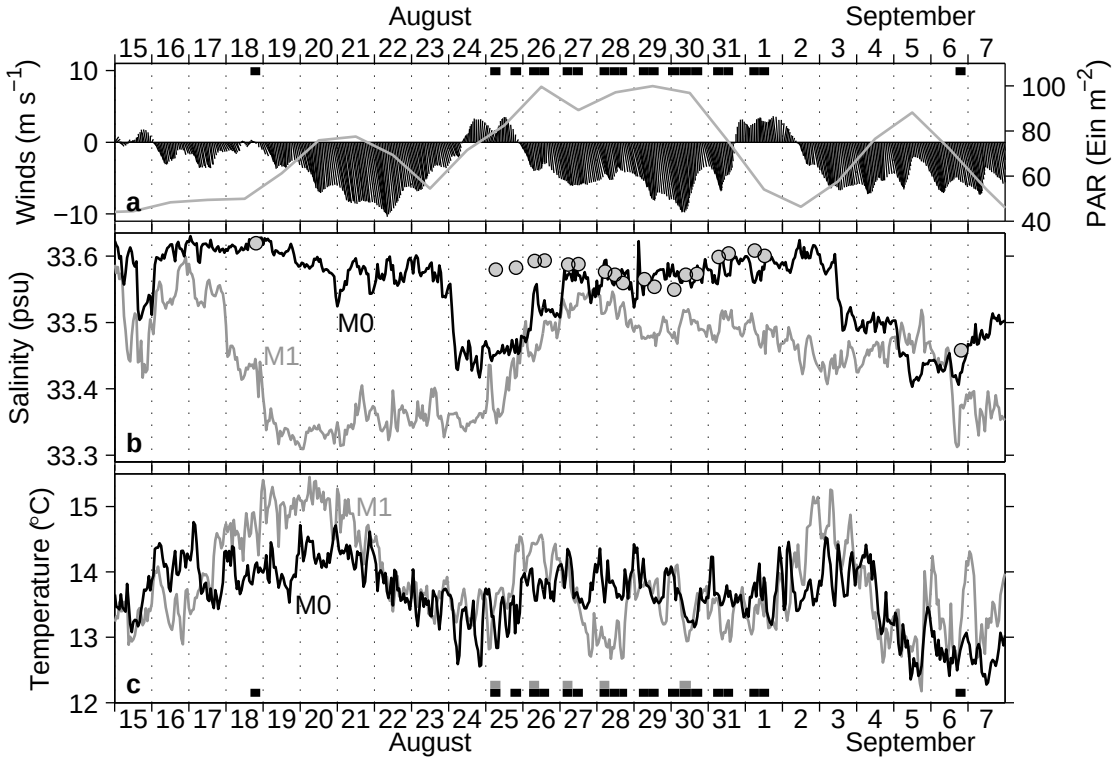
August
September
15 16 17 18 19 20 21 22 23 24 25 26 27 28 29 30 31 1 2 3 4 5 6 7
Winds (m s^{-1})
10
0
−10
a
PAR (Ein m^{-2})
100
80
60
40
Salinity (psu)
33.6
33.5
33.4
33.3
M0
M1
b
Temperature (°C)
15
14
13
12
M1
M0
c
15 16 17 18 19 20 21 22 23 24 25 26 27 28 29 30 31 1 2 3 4 5 6 7
August
September

Figure 3

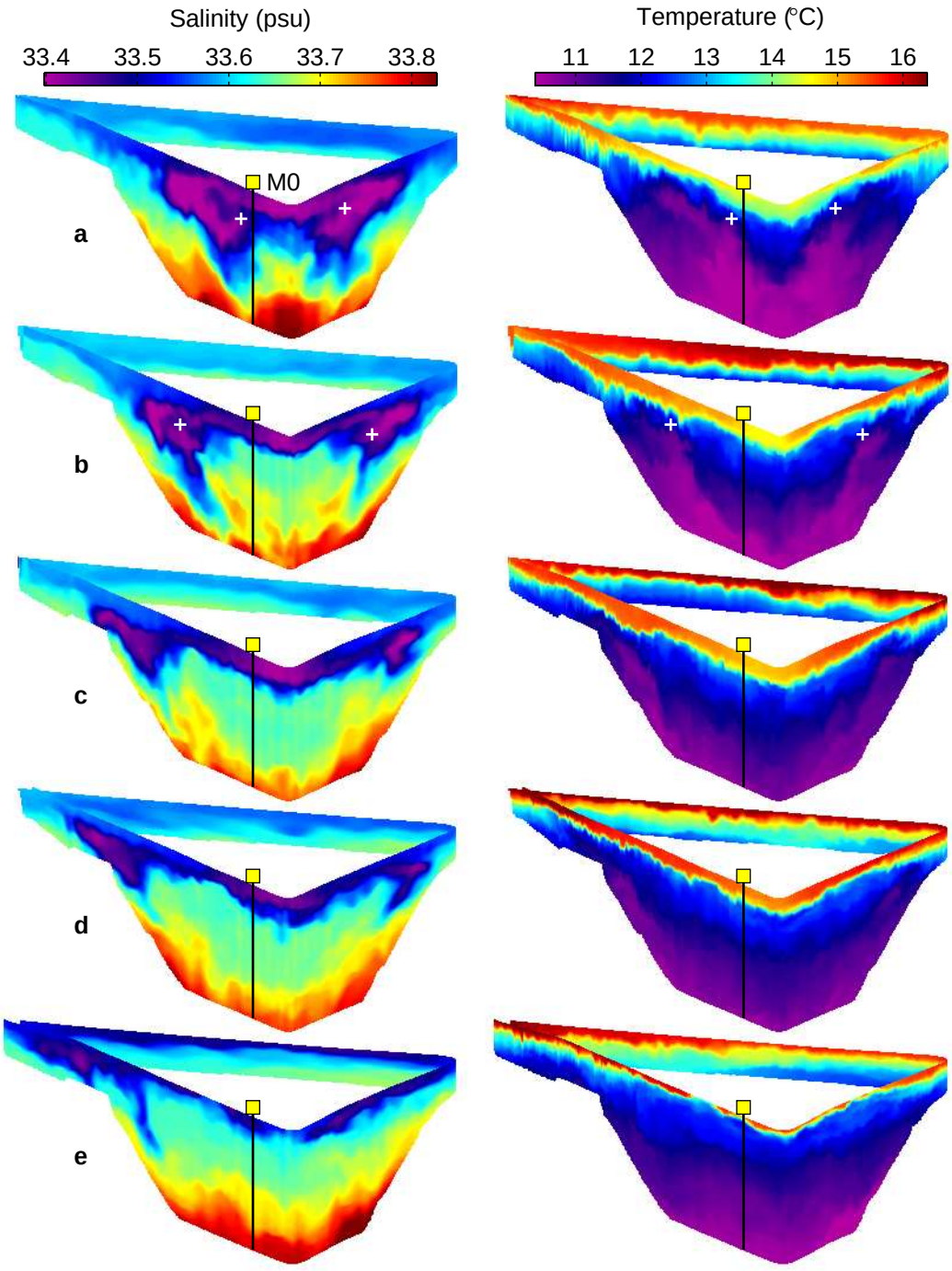
Salinity (psu)
33.4
33.5
33.6
33.7
33.8
Temperature (°C)
11
12
13
14
15
16
M0
a
b
c
d
e

Figure 4

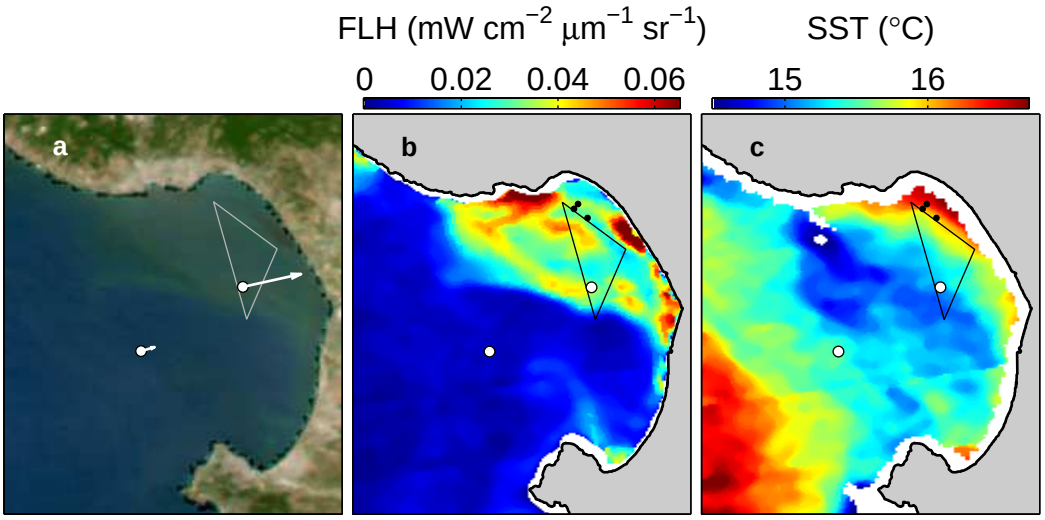

Figure 5

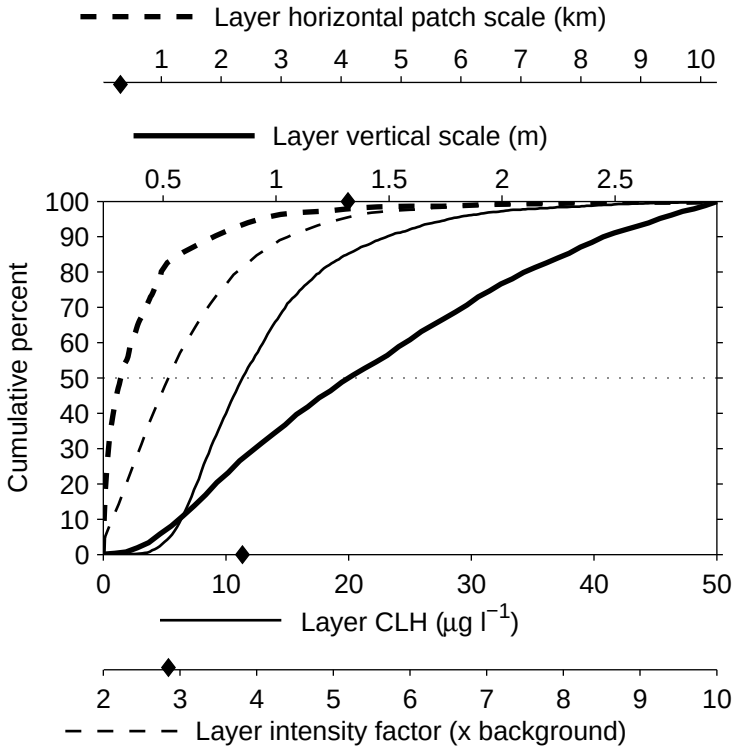
Layer horizontal patch scale (km)
1 2 3 4 5 6 7 8 9 10
Layer vertical scale (m)
0.5 1 1.5 2 2.5
Cumulative percent
100 90 80 70 60 50 40 30 20 10 0
0 10 20 30 40 50
Layer CLH (µg l−1)
2 3 4 5 6 7 8 9 10
Layer intensity factor (x background)

Figure 6

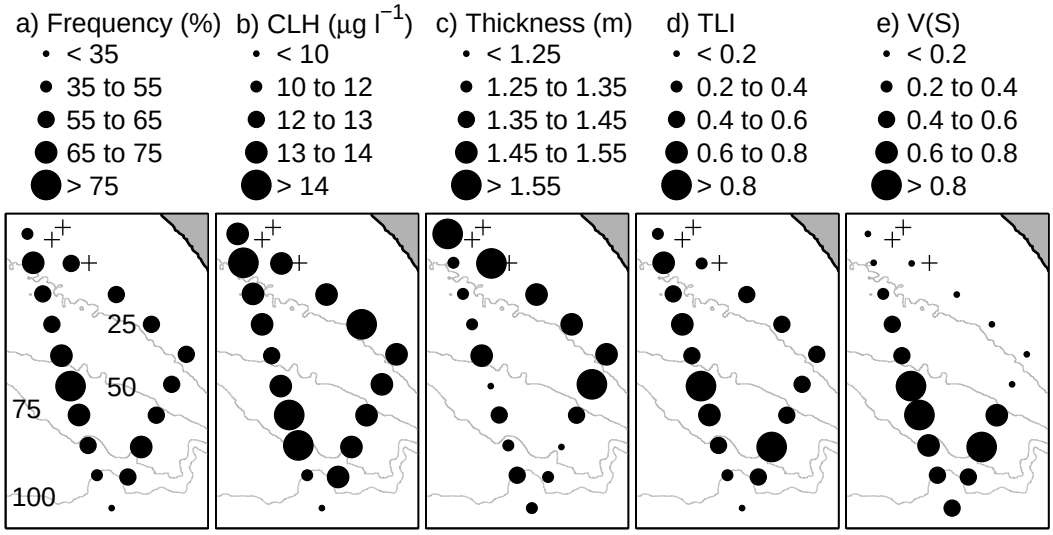
a) Frequency (%)
< 35
35 to 55
55 to 65
65 to 75
> 75
b) CLH (µg l^{-1})
< 10
10 to 12
12 to 13
13 to 14
> 14
c) Thickness (m)
< 1.25
1.25 to 1.35
1.35 to 1.45
1.45 to 1.55
> 1.55
d) TLI
< 0.2
0.2 to 0.4
0.4 to 0.6
0.6 to 0.8
> 0.8
e) V(S)
< 0.2
0.2 to 0.4
0.4 to 0.6
0.6 to 0.8
> 0.8
25
50
75
100

Figure 7

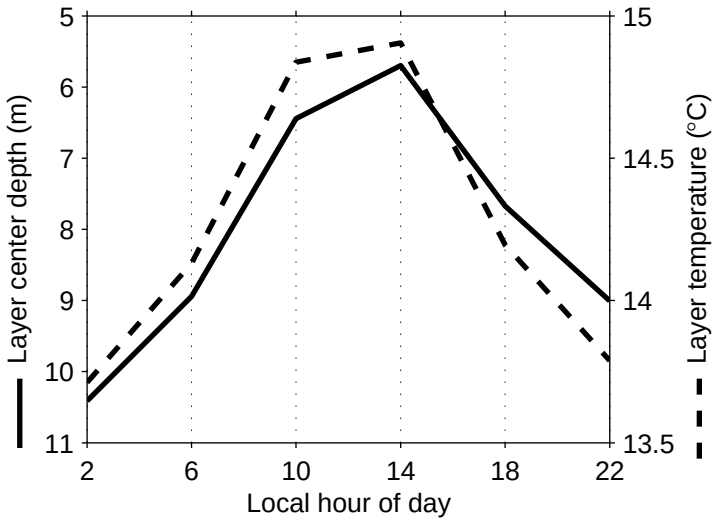
5
6
7
8
9
10
11
Layer center depth (m)
15
14.5
14
13.5
Layer temperature (°C)
2
6
10
14
18
22
Local hour of day

Figure 8

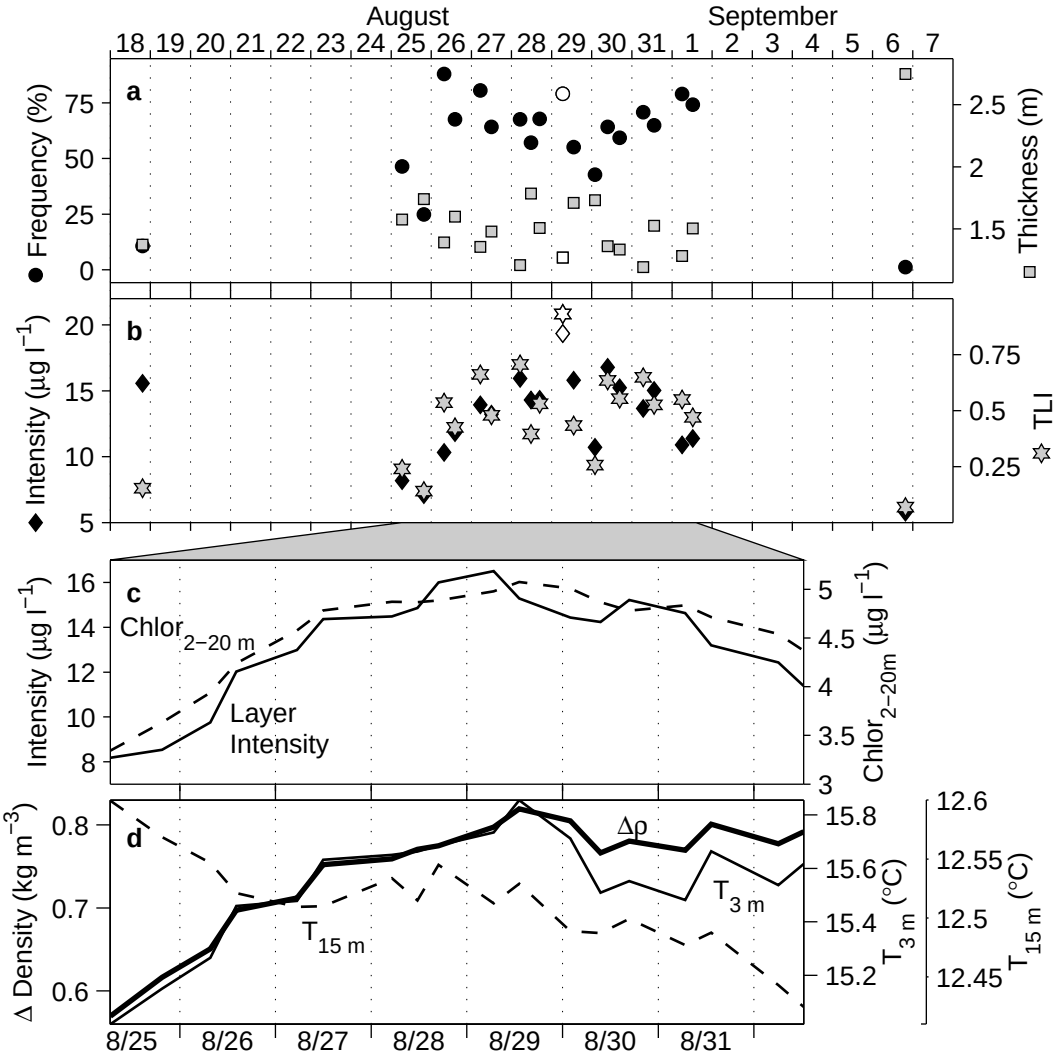
August
September
18 19 20 21 22 23 24 25 26 27 28 29 30 31 1 2 3 4 5 6 7
a
Frequency (%)
Thickness (m)
b
Intensity (µg l−1)
TLI
c
Chlor2−20 m
Layer Intensity
Intensity (µg l−1)
Chlor2−20m (µg l−1)
d
Δ Density (kg m−3)
Δρ
T15 m
T3 m
T3 m (°C)
T15 m (°C)
8/25 8/26 8/27 8/28 8/29 8/30 8/31

Figure 9

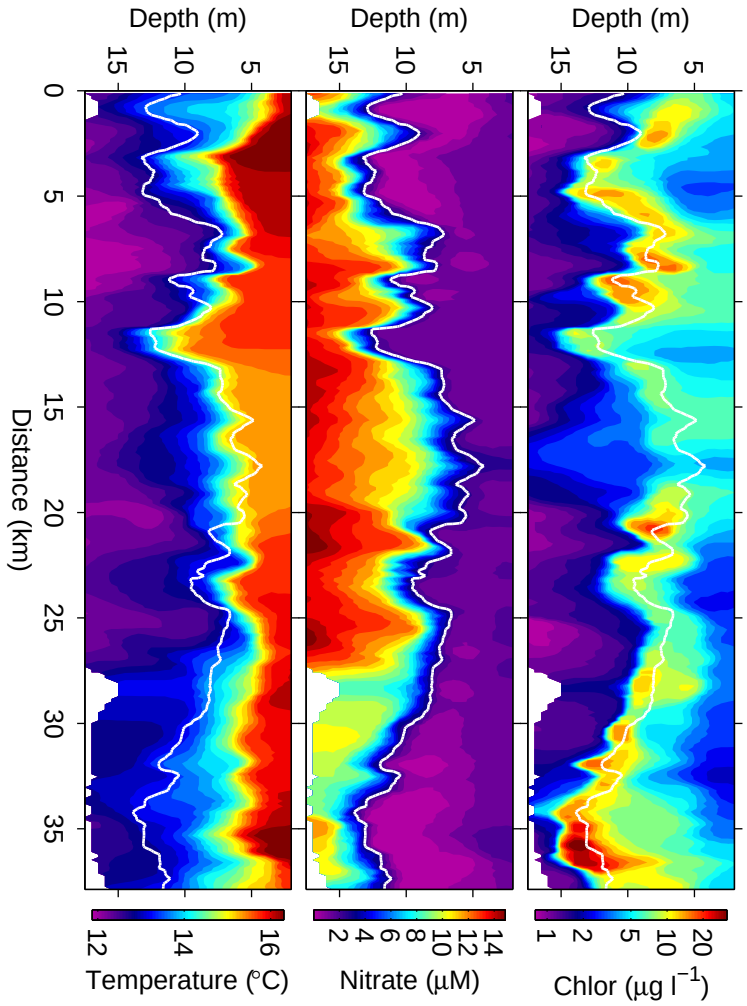
Depth (m)
Depth (m)
Depth (m)
15
10
5
0
5
10
15
20
25
30
35
Distance (km)
12
14
16
Temperature (°C)
2
4
6
8
10
12
14
Nitrate (µM)
1
2
5
10
20
Chlor (µg l−1)

Figure 10

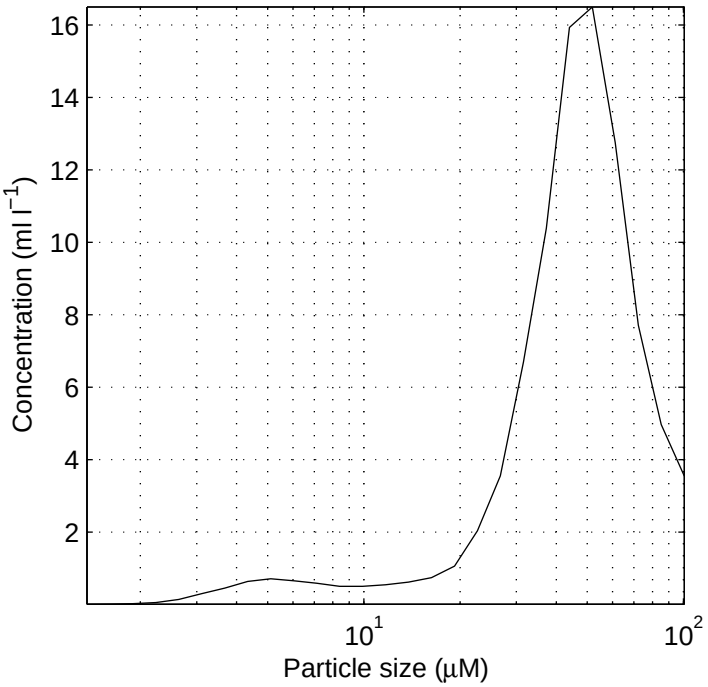

Figure 11

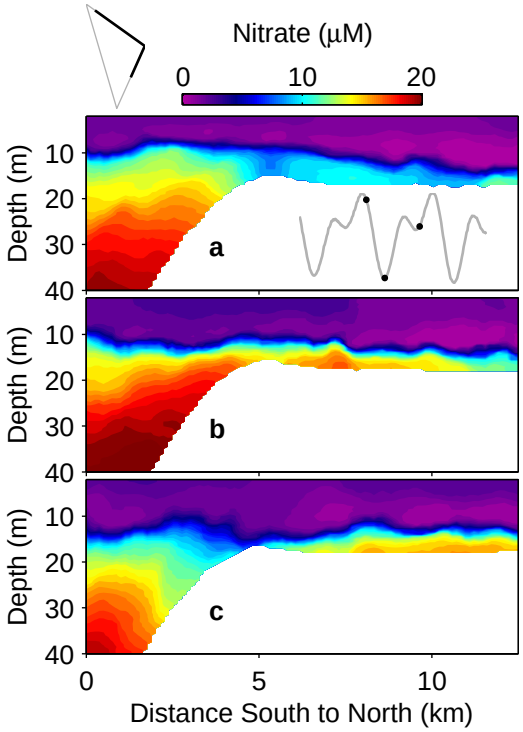
Nitrate (µM)
0
10
20
Depth (m)
10
20
30
40
a
b
c
0
5
10
Distance South to North (km)